Assessing the role of adhesives in durability of laminated veneer lumber (LVL) by fracture mechanics

Babak Mirzaei, Arijit Sinha, and John A. Nairn
Wood Science & Engineering, Oregon State University, Corvallis, OR 97331

DOI 10.1515/hf-2015-0193
Received September 10, 2015, accepted January 25, 2016

Abstract: This study explored the use of fracture toughness properties for durability assessment of wood composite panels. The main objective was to develop a new method for ranking the role of adhesives in the durability of wood-based composites by observing changes in fracture toughness during crack propagation following cyclic exposure to moisture conditions. We compared this new approach to conventional mechanical performance test methods, such as observing strength and stiffness loss after exposure. Comparing changes in fracture toughness as a function of crack length after moisture cycling shows that fracture-mechanics based methods can distinguish different adhesive systems on the basis of their durability, while conventional test methods do not have similar capability. Using steady-state toughness alone, the most and least durable adhesives (polyvinyl acetate and phenol formaldehyde) could be distinguished, but the performance of two other adhesives (emulsion polymer isocyanate and phenol resorcinol formaldehyde) could not. Further analysis of experimental *R* curves (toughness as a function of crack length) based on kinetics of degradation was able to rank all adhesives confidently and therefore provided the preferred method. The likely cause for the inability of conventional tests to rank adhesives is that they are based on initiation of failure while the fracture tests show that comparisons that can rank adhesives require consideration of fracture properties after a significant amount of crack propagation has occurred.

Keywords: crack propagation fracture toughness, cyclic moisture conditions, 3D digital image correlation (DIC), double cantilever beam (DCB) fracture test, durability assessment, emulsion polymer isocyanate (EPI), laminated veneer lumber (LVL), phenol formaldehyde (PF) resin, phenol resorcinol formaldehyde (PRF) resin, polyvinyl acetate (PVA) resin, R curve, toughness, vacuum pressure soaking drying (VPSD) cycle, wood adhesives

Introduction

The ideal experiment for assessing durability of a product is to fabricate actual-sized specimens, subject them to actual service loads (either loads or moisture), and then periodically monitor their residual properties. This "ideal" approach is impractical for several reasons. First, the experiments are too time consuming; it may take a long time for specimens to show effects under actual service loads. Second, most durability experiments are highly variable making it difficult to gain any statistical confidence in the results (Sinha *et al.* 2012). The solution is to develop accelerated methods that can give useful information about durability in shorter-term tests.

Typical wood-based composite tests for moisture durability operate by exposing products to wet and/or hot environments and then inspecting for signs of damage (*e.g.*, ASTM D2559 or D1037). Such tests are often qualitative (*e.g.*, pass/fail based on observation of damage). These tests can be made quantitative by coupling with suitable mechanical tests. For example, static bending and shear tests are common methods for

evaluating the resistance of wood-based composites to aging. While the former supposedly addresses material durability as a whole, the latter aims to evaluate the quality of the bond-line after accelerated aging (ASTM D1037 2012, NIST Standard 2010). Unfortu-nately, these common tests look only at early stages of loading up to initiation of failure. These properties do not depend strongly on the adhesive and therefore are poor tests for ranking adhesives (Stoeckel *et al*. 2013). In contrast, it was recently shown that fracture analysis of crack propagation within a single composite material (OSB, plywood, LVL, *etc*.) provides more information than conventional bond stiffness and strength testing (Sinha *et al*. 2012). For example, the increase in toughness for LVL specimens during crack growth contains a large contribution from the adhesive (Mirzaei *et al*. 2015).

Our goal was to develop a methodology for quantitative assessment of wood adhesives that can predict which ones provide advantages for moisture durability. Our hypothesis was that a good approach would be to combine exposure experiments with fracture property characterization. Furthermore, the fracture property experiments should include fracture toughness changes during crack propagation to include information beyond the initiation stage. In other words, we explored expanded use of fracture toughness as a design tool for durable wood composite panels. The key experiment was to look for correlations between fracture toughness and durability by parallel fracture and durability experiments. If successful, fracture tests could be proposed as an accelerated method for ranking adhesives and designing durable composite panels. The same approach was used for accelerated testing of aerospace composites by monitoring microcracking fracture toughness during hydrolytic degradation experiments on aerospace composites (Kim *et al*. 1995, Han and Nairn 2003). This approach was a great improvement over pass/fail methods that were previously used by Boeing. A similar approach was also used to assess high-temperature performance of wood-based composites (Sinha *et al*. 2012). The fracture properties helped identify which composites were most susceptible to thermal damage.

The new aspects of this study were to compare different adhesives and to focus on moisture durability. We assessed the durability of four conventional adhesive systems used for Laminated Veneer Lumber (LVL). The main task was to develop methods for analyzing observed changes in fracture toughness during crack propagation following cyclic exposure to moisture conditions in order to rank adhesives for durability. We compared these new methods to conventional mechanical performance test methods such as observation of strength and stiffness loss after exposure. An advantage of the new methods is that they extend into the post-peak regime while conventional methods focus on pre-peak response (for stiffness loss) or peak load only (for strength loss). The additional information in the post-peak regime can help compare adhesives. Finally, several data analysis methods were examined in order to determine which method provides the best information for adhesive comparisons.

Materials and methods

Materials: LVL billets were manufactured in the laboratory under controlled conditions using all B-grade Douglas-fir veneers. Each LVL billet had dimensions 61cm X 91cm (2ft X 3ft), consisted of 11 plies (each 3 mm thick), and one of the following four adhesives: Wonderbond® EL-35 Emulsion Polymer Isocyanate (EPI), GP® 421G83 RESI-MIX® Phenol Formaldehyde (PF), CASCOPHEN® LT-5210J/ CASCOSET® FM-6210 adhesive system Phenol Resorcinol Formaldehyde (PRF), and a one-component Polyvinyl Acetate (PVA). Glue spread rate (coverage of 250-300 g/m^2) and press conditions were adjusted according to the guidelines of the relevant adhesive manufacturer. PVA billets were pressed at 2.07 MPa (300 psi) at room temperature for about 1 hour. PF billets were pressed at 0.69 MPa (100 psi) for 5 minutes at room temperature and then hot-pressed at 2.07 MPa (300 psi) for 20 minutes at

180°C. EPI and PRF billets were pressed at room temperature at 0.83 MPa (120 psi) for 20 minutes and 8 hours, respectively.

After pressing, the LVL billets were conditioned in a standard room maintained at 20°C, 65% RH for one week before further testing. Note that commercial LVL normally uses high-grade veneers on the surfaces and low-grade veneers in the middle (Wang and Dai 2005). For this work, however, it was important to have uniform grade veneer throughout.

Moisture Treatment: Accelerated moisture exposure was carried out according to ASTM Standard D2559, but we excluded the steam exposure step. Each cycle started by exposing the samples to 85 kPa vacuum for 5 minutes followed by submersion in water in a pressure vessel at 517 kPa for 1 hour. After removal from the pressure vessel, the samples were oven-dried at 65 ± 2° C for 21-22 hours (ASTM D2559 2012). These steps represented one moisture cycle or vacuum pressure soaking drying (VPSD) cycle. Samples were subjected to 0 (for controls), 8, 16 and 24 cycles. After these selected numbers of cycles, samples to be tested were thoroughly dried at 103° C for 24 hours and then stored in the standard conditioning room until they reached equilibrium. After reaching equilibrium, the samples were tested for fracture properties and for stiffness and strength properties.

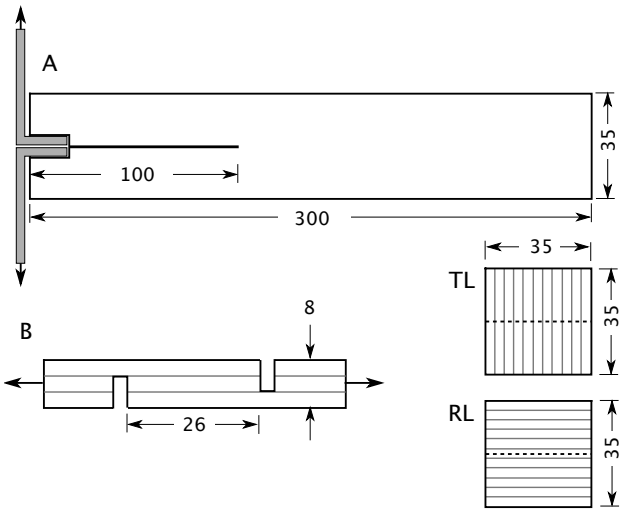

Figure 1: (a) The double cantilever beam specimen (DCB) used for crack propagation experiments. The TL and RL diagrams on the lower right show end view of those specimens with gray lines indicating bond lines between veneers and the dashed line indicating the crack propagation plane. (b) The 3-ply, lap shear specimen used for conventional shear strength tests by loading in tension. All dimensions are in mm.

Crack Propagation Experiments: The toughness or critical energy release rate for a material is the amount of energy released by unit increment in new crack area (Irwin 1958). For some materials, including wood, this critical energy changes as the crack propagates. An experimental measure of this change is known as the crack resistance curve, or *R* curve. *R* curves can be measured from experimental data for load, displacement, and crack length by integrating load-displacement data up to some point for which crack propagation data is available and then dividing the incremental released energy by newly created fracture surface area (Nairn 2009).

Wood can be considered as an orthotropic material with three perpendicular material directions, namely, longitudinal (L), tangential (T), and radial (R). For LVL specimens, T and R refer to tangential and radial direction of wood in the veneer layers, which correspond to in-plane and thickness direction of the rotary-peeled veneers, respectively. Accounting for this anisotropy, six crack propagation systems can be defined, *i.e.*, TL, RL, LR, TR, RT and LT (Smith *et al*. 2003). The first letter stands for the normal to crack plane while the second indicates the propagation direction. In the present study, all fracture tests were either TL or RL crack propagation.

A TL crack in LVL spans all adhesive bond lines while an RL crack plane would be parallel to the bond lines (see Fig. 1). Our first experiments looked at both RL and TL fracture. For solid wood, the TL *R* curve rises more than the RL. In LVL the differences are dramatic with much greater rise in *R* curve for TL compared to RL fracture and with much higher toughness than solid wood (Mirzaei *et al*. 2015). The significantly higher TL *R* curves for LVL indicate more contribution of adhesive to TL fracture compared to RL fracture. In RL crack growth, the crack may propagate along a single bond line or may deviate into the wood within a single veneer layer. Hence, RL fracture may not provide sensitive information on adhesion quality. In contrast, TL cracks span all adhesive bond lines in the specimen. Such cracks will always break bond lines and veneers. Because of this greater role of adhesive in TL fracture, all crack propagation experiments reported here for LVL were in the TL direction.

Crack propagation fracture toughness tests were carried out using an energy method developed for

direct *R* curve measurement (Nairn 2009). More specifically, crack propagation experiments were conducted using double cantilever beam (DCB) specimens that were cut from equilibrated LVL billets (see Fig. 1). The initial cracks were cut with a band saw for TL fracture tests. To avoid possible weak adhesion zones near the edges, the edges of the LVL billets were marked before sawing and the initial specimen cracks were cut from the marked ends, such that all cracks propagated away from the edges. Hence, the quality of the inner zone adhesion was tested. Dimensions of all DCB samples were $35 \pm 2 \times 35 \pm 2 \times 300 \pm 5$ mm^3 and the initial, sawn pre-crack was 100 mm.

The samples were tested in an Instron 5582 universal testing machine. Load and displacement data were continuously recorded during tests. The DCB fracture tests were conducted in opening mode under displacement control at 2 mm/min. The crack plane at the edge of each specimen was widened and loading was applied using angle irons inserted into the gap. Crack growth data were collected using the 3D Digital Image Correlation (DIC) technique. Mirzaei *et al*. (2015) has successfully demonstrated the use of DIC techniques for crack propagation in wood. Similar techniques were used in this study. A brief description is provided here, but a detailed description on DIC implementation for crack data population can be found in a previous paper (Mirzaei *et al*. 2015). DIC is a technique to map strains by tracking a small subset of pixels in deformed images. It is especially useful for materials whose surface cannot be polished, such as wood. The tensile strain normal to the crack plane ahead of the crack tip was monitored throughout the loading. Crack propagation was measured by observing shifts in the position to reach 1% vertical strains between subsequent images.

Replicate specimens (8±2 for PVA LVL and 6±2 for the rest) were used to evaluate each moisture exposure condition. Each specimen gave an *R* curve. To average multiple *R* curves, we determined a common range for the average curve by performing interpolation/extrapolation on each curve to get new datasets with a common set of crack length points, followed by averaging the corresponding interpolated toughness values. Standard deviations of toughness were computed for each crack increment and plotted along with averaged *R* curves. For additional statistical analysis, two-way Analysis of Variance (ANOVA) tests were carried out to account for the effect of crack growth, accelerated aging, and their interaction on fracture toughness.

Conventional Strength and Stiffness Testing: Parallel stiffness and strength tests were carried out for comparison to toughness results. Modulus of elasticity *E* can be computed from DCB arm bending using the following beam equation:

$$E = \frac{8Pa^3}{\delta b h^3}$$

where, P/δ is slope of the load *vs*. crack opening displacement curve before the proportional limit, *a* is initial crack length, *b* is beam breadth and *h* is height of the beam arm. This modulus, however, needs correction due to shear and crack tip arm rotation, especially because the length to depth ratio of the arms (a/h ~ 6) was rather small. The correction can be done by replacing crack length, a, with an effective crack length $a+\chi h$, where χ is a correction factor. A correction factor developed for uniaxial fiber-polymer composite can be applied to wood-based composites using the following equation (Hashemi *et al*. 1990):

$$\chi = \sqrt{\frac{E_L}{11G_{LT}}\left(3 - 2\left(\frac{\Gamma}{1+\Gamma}\right)^2\right)}$$

where, $\Gamma = 1.18\sqrt{(E_L E_T)}/G_{LT}$. E and G are the elastic moduli in the appropriate directions approximated using solid Douglas-fir elastic properties provided by US Forest Products Laboratory (2010) as $E_L = 13$ GPa, $E_T = 0.65$ GPa and $G_{LT} = 1.01$ GPa. The moduli were found for each DCB specimen and therefore had the same number of replicates as the fracture tests.

For a strength-based test, notched 3-ply shear specimens were cut from the arms of the DCB samples after fracture tests to test the same material that was exposed to the same weathering conditions as the fracture specimens. Because the arms do not sustain damage during fracture tests the material in those arms can provide suitable comparison specimens. A shear test (NIST Standard 2010) was conducted using an Instron 5582 universal testing machine. The shear area needed to find the shear stress was measured for each specimen using calipers. The test configuration and nominal dimensions are shown in Fig. 1. Shear test results consisted of 6±2 replicates for each condition.

Results and discussion

LVL samples made using EPI, PVA, PRF and PF adhesives and B-grade Douglas fir veneers were tested for fracture toughness during crack propagation. The resulting *R* curves for control specimens and specimens exposed to 8, 16, and 24 VPSD cycles are in Fig. 2. Each curve is the average of several replicates. With the error bars indicating standard deviations. All *R* curves show typical behavior with initiation toughness (G_{init}), which was a relative low toughness and comparable to the initiation toughness of solid wood (100 to 300 J/m^2), followed by an increase in toughness as a function of crack length. Most curves approached a steady-state toughness, G_{ss}, at high crack growth. After reaching steady state toughness, deviations from the resulting plateau are likely due to either edge effects or to material inhomogeneity. The *R* value is determined from $R = (1/t)dU/da$ were *U* is total energy released up to crack length *a* and *t* is thickness. As the crack approaches the edge of the specimen, however, the crack slows down and *da* approaches zero, which can cause *R* to become large and unreliable (Matsumoto and Nairn 2012). As a result, the rises at long crack length were attributed to edge effects. After reaching steady state, the fracture toughness does not normally drop in homogeneous materials, however, in wood or wood composites, a crack may enter a weak zone affecting material's toughness. It is important to recognize that the B-grade veneer used for LVL fabrication in this study may have some weak zones.

The plot scales in Fig. 2 were adjusted to be the same for all materials (with PVA as the one exception) for ease of comparison. The PF, PRF, and EPI adhesives seem to equally contribute to the fracture energy of the materials in the control condition, hence, creating roughly equal *R* curves. In contrast, the control *R* curve for PVA was higher and reached higher G_{ss} at longer critical crack length. The one-component PVA used in this study was the only adhesive without any considerable crosslinking capability. The high

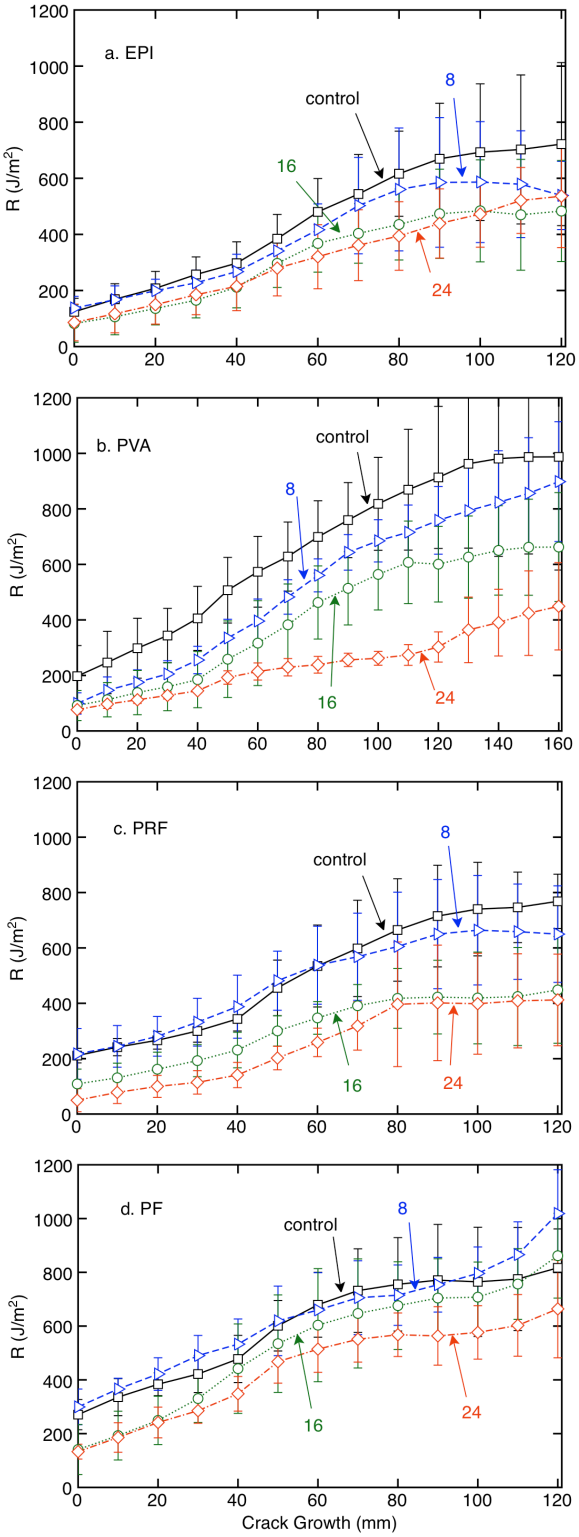

Figure 2: Average fracture *R* curves of LVL made using a. EPI, b. PVA, c. PF and d. PRF adhesives exposed to 0, 8, 16, and 24 VPSD cycle treatments (as indicated on each plot). Note that x-axis scale on b. PVA differs from the other three plots.

fracture toughness maintained by PVA can be attributed to additional flexibility of linear molecular chain segments, as compared with the more brittle behavior of the other adhesives with cross-linked molecular structures (Suzuki and Schniewind 1987). That being said, we did not observe as much contrast among the adhesives in terms of their fracture toughness when bonded to wood as some other studies have reported, but those studies did not carry out a full *R* curve analysis. Most prior work did fracture tests on the bond-line, which corresponds to RL fracture instead of the TL fracture used here. Additionally, they reported only initiation toughness or total work of fracture. Pizzi and Mittal (2003) have collected these results.

The crack length at which toughness becomes constant is a measure of the size of the fiber-bridging zone that develops in the wake of the crack propagation. Once the bridging zone is fully developed, additional crack growth will be at constant bridging zone length and constant G_{ss} (Nairn 2009). According to Fig. 3, the fiber bridging zone is roughly 130 mm for PVA-made LVL while it is about 90 mm for LVL made with other adhesives. Fracture toughness at these crack lengths were considered to be G_{ss} for that material. Exposure to accelerated aging (VPSD cycles) caused G_{ss} to decrease and also affected other toughness attributes such as the G_{init} and the *R* curve shape. *R* curve shape can be translated into bridging stress distribution (Gallops 2011) as a measure of the ability of those fibers in combination with adhesive to increase toughness. Quantitative interpretation of *R* curve shape requires numerical modeling and will be covered in a future publication. This work looked at various changes in experimental features of the *R* curves to find the preferred assessment criterion for ranking the ability of adhesives to provide durable wood composites.

According to Fig. 2, *R* curves clearly showed degradation as a function of accelerated aging cycles. According to the results of a two way ANOVA, fracture toughness significantly increases as a function of crack propagation ($p < 0.05$). It also significantly deteriorates due to aging ($p < 0.05$). However, the interaction of aging and crack growth on toughness was not statistically significant.

For each durability indicator studied, our comparisons used percentage property retention defined as the property after aging normalized to the control property (and expressed as a percentage). This approach gives emphasis to degradation trends due to aging. Additionally, the comparison can be carried out among various properties to choose the most suitable durability indicator. We also compared the degradation trends of toughness properties to degradation trends measured using conventional strength and stiffness properties. These conventional properties are based on initial slope (stiffness) or on load at initiation of failure (strength) and therefore, do not take into account any experimental results after crack propagation.

The first toughness property to consider was the initiation toughness or G_{init}. For materials with fiber bridging zones, such as wood and LVL, G_{init} is less than G_{ss} and may be signifycantly less as determined by material's toughening capacity. It has been observed that G_{init} of solid wood and PVA LVL made out of the same species are roughly the same, but their G_{ss} levels are considerably different (Mirzaei *et al*. 2015). Even after aging, the decreases in solid wood and LVL G_{init} values are similar indicating minimal contribution of adhesive to the initiation of fracture (Mirzaei *et al*. 2015). Besides PVA LVL, the results here showed inconsistent decreases in G_{init} as a function of aging for EPI, PRF, and PF made LVL (see Fig. 2). In brief, it is likely that the G_{init} of LVL is determined predominantly by solid wood properties, which implies that G_{init} is not a proper indicator for assessing the role of adhesive in durability.

In contrast to G_{init}, G_{ss} is the toughness of the material after the full development of bridging zones. In the steady-state regime, the size of the bridging zone is constant (it propagates along with crack growth) and therefore, toughness become constant as well. As suggested by the

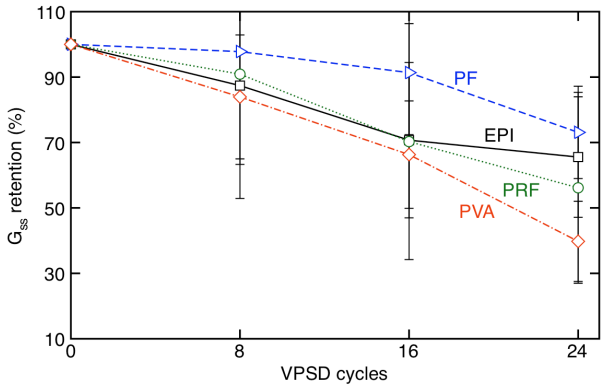

Figure 3: Steady state toughness (G_{ss}) retention of various adhesives as a function of the number of VPSD cycles.

larger increase in toughness of LVL compared to solid wood, adhesives considerably promote the contribution of fiber bridging to LVL toughness (Mirzaei *et al*. 2015). As a result, G_{ss} should relate to adhesive quality. The retention of G_{ss} for the various adhesives as a function of aging is shown in Fig. 3. The materials clearly varied in terms of durability performance. G_{ss} constantly declined due to aging for all adhesives. The PVA-made LVL relatively lost the most toughness, while PF-made LVL lost the least (or maintained toughness the most). For both PF and PVA, the degradation observed due to exposure from 16 to 24 VPSD cycles was the sharpest, hence, the deterioration effect in the final cycles was the most severe. The average retention after the final cycle is approximately 73% and 40% for PF and PVA, respectively. Based on this plot, the most and least durable adhesives, *i.e.*, PF and PVA, can be detected, but no judgment can be made regarding the durability of EPI *vs*. PRF.

Kinetics of Toughness Degradation

To distinguish adhesives further, we looked at the rate of degradation at different crack lengths. First, we assumed a simple first-order kinetics analysis based on an assumption of water causing some sort of hydrolysis degradation:

$$\frac{dR(\Delta a)}{dt} = -K(\Delta a, T)[\mathrm{H_2O}](t)$$

where $R(\Delta a)$ is toughness at crack length Δa, $K(\Delta a,T)$ is a rate constant that may depend on crack length (*i.e.*, the extent of adhesive involvement) and temperature (*i.e.*, though an activation energy) and $[H_2O](t)$ is the time-dependent concentration of water. Integrating this equation gives

$$\begin{aligned} R(\Delta a) &= R_0(\Delta a) - K(\Delta a, T)\int_0^t [\mathrm{H_2O}](t)dt \\ &= R_0(\Delta a) - k(\Delta a, T)t \end{aligned}$$

where $R_0(\Delta a)$ is the toughness before aging. Because the integrated moisture concentration should be the similar for wood samples exposed to identical moisture conditions, that term can be rolled into an effective rate constant, $k(\Delta a,T)$, which can be found from the slope of $R(\Delta a)$ *vs*. cycle number at constant crack growth (Δa). Sample fracture toughness degradation plots for PVA LVL at 50 to 110 mm crack propagation along with linear degradation rate fits are presented in Fig. 4. In brief, this 3D figure shows scatter plot of individual experimental results for different crack growth and different numbers of cycles. To calculate degradation rates, we considered all combinations of points for a given

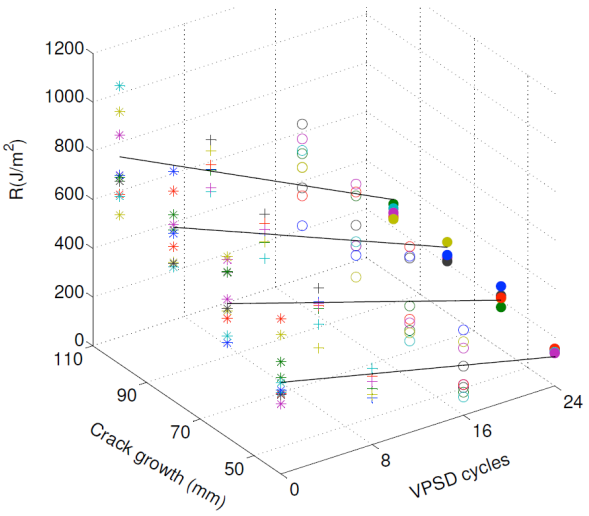

Figure 4: Fracture toughness degradation rates of PVA LVL at 50-110 mm of crack propagation. The symbols are individual experiments. The lines are fits using our error analysis procedure.

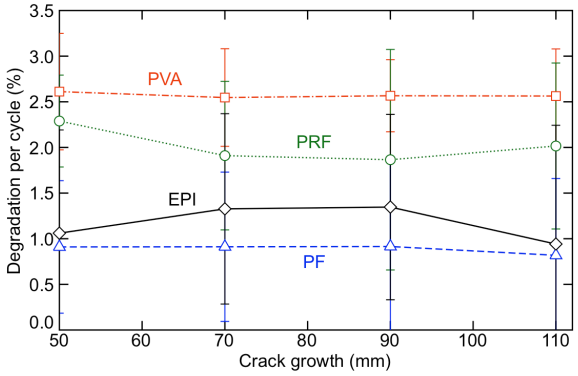

Figure 5: The rate of degradation of toughness (due to hydrolysis) for each adhesive calculated at different amounts of crack growth. The error bars are standard deviations to the rates as estimated by our error analysis procedure.

Δa, found $k(\Delta a,T)$ for each set, and normalized by intercept to get relative toughness degradation rates. For error analysis results, we found average and standard deviations of those normalized rates. The lines in Fig. 4 are plots using the averaged slopes. Finally degradation rates for all adhesives at 50 to 110 mm of crack propagation and normalized to initial toughness are plotted in Fig. 5 together with error bars determined from the above error analysis. Because of the unsuitability of G_{init}, all these results are for after some crack propagation. Additionally, after some crack growth the degradation trends tend to become flat making ranking of the adhesives easier. Welch's t-tests were done to statistically compare all adhesives one by one at each crack size. According to the results, the durability differences shown in Fig. 5 are significantly different at most crack sizes ($p < 0.05$). The smallest degradation rate, indicating the highest durability, is associated with PF while the largest degradation rate is associated with PVA. This result is in agreement with Fig. 3 based on G_{ss}. Kinetics analysis helps distinguish adhesives further. According to the results of this study, LVL composites made using PF, EPI, PRF and PVA adhesives and the same wood species, are ranked in terms of durability in that order with PF being the most durable. Using G_{ss} alone the boundaries (PVA and PF) could be established, but EPI and PRF could not be distinguished. Kinetics analysis allows for differences to be observed in the durability performances of EPI and PRF, making this a preferred method to rank adhesive performance in a composite panel.

Conventional Durability Indicators

Strength and stiffness tests were carried out in parallel and the outcomes were compared to the fracture toughness results. Based on shear strength retention results (Fig. 6a), the adhesives are indistinguishable within the scatter of the results. Although a general shear strength decline due to aging can be observed, the scatter in the results renders any statistical comparison inconclusive. While parallel to grain shear strength tests have relatively small COV (14%) in clear wood (Liswell 2004), our shear strength tests had

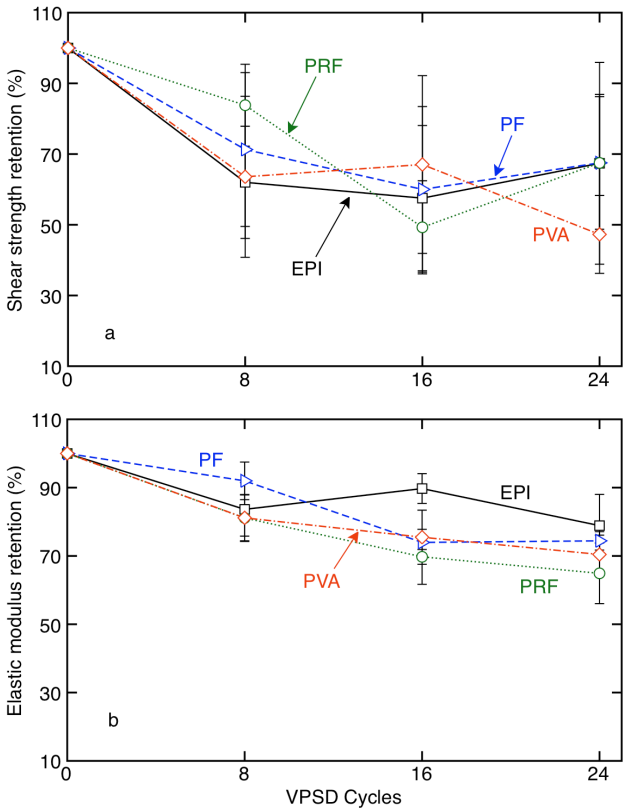

Figure 6: a. The retention in shear strength from lap shear tests for each adhesive as a function of the number of VPSD cycles. b. The retention in modulus measured from initial stiffness of DCB specimens as a function of the number of VPSD cycles.

higher COV (up to 42%). Because both wood and adhesive failures can occur in bond strength tests of wood composites, the scatter of such tests is usually higher, which complicates interpretation of the results. Overall, adhesive performance cannot be differentiated based on shear strength results. Follrich *et al*. (2010) compares the moisture durability of PRF and EPI wood bonds using internal bond strength tests before and after 24 cycles of accelerated aging and reported a marginally better performance for PRF. They also reported, however, that the wood failure area considerably decreased in PRF-bonded specimens after accelerated aging while in EPI-bonded specimens the trend was reverse. These observations indicate better performance for EPI. The inconsistency in their results between strength tests and wood failure area observation corroborates the shortcomings of conventional bond durability tests based on strength.

The modulus retention, as calculated from corrected DCB stiffness, is plotted in Fig. 7. The DCB modulus correction factor, χ, was found to be relatively large, about 1.45, for the studied materials indicating the necessity of modulus correction. The corrected DCB modulus method was randomly verified by comparison to standalone 3-point bending modulus tests that were also corrected for shear. For example, the ratio of corrected moduli in 3-point bending to corrected DCB modulus was found to be 1.03 for untreated PVA LVL and 1.1 for PVA LVL after 8 VPSD cycles. In brief, the modulus determined from initial DCB stiffness gave good results for actual LVL modulus. Except for EPI, other adhesives exhibited constant degradation in modulus as a function of aging, however, there is no clear distinction among the adhesives. Similar to shear strength, stiffness merely demonstrates general degradation due to aging. Modulus had smaller error bars compared to toughness and shear strength experiments, but the change in modulus was too similar among the tested resins for modulus results to help in distinguishing durability of those resins. Similar modulus and strength effects were reported for plywood, another laminated composite (MacLean 1953, Kojima and Suzuki 2011, Sinha *et al*. 2011). In particulate composites, however, such as particleboard, stiffness seems to be affected by aggressive environments more than strength (MacLean 1953, Kojima and Suzuki 2011, Sinha *et al*. 2011).

The likely cause for the inability of shear and stiffness tests to rank adhesives is that they are based on initiation of failure or, in the case of stiffness, on pre-failure properties. Our fracture tests in the post-failure regime show that much better comparisons come only after a significant amount of crack propagation.

Adhesive Bond Microscopy

To examine the studied adhesives further, we looked at bond line characteristics through bright field and Ultra Violet (UV) microscopy. Micrographs are presented in Fig. 7. While PF shows a considerable interphase region where adhesive penetrates the wood cells, PVA shows almost no penetration into the substrate. This result agrees with the X-ray analyses of wood adhesive bond lines (Kamke *et al*. 2014). According to the durability assessment results of wood adhesives obtained by crack propagation fracture experiments, PF and PVA are respectively the most and least durable adhesives studied here. PF was the only adhesive requiring high temperature for curing which may have helped to increase adhesive penetration. PRF seems to have slightly larger wood interphase than EPI and has been reported to penetrate into wood only about 20% more than PVA (Adamopoulos *et al*. 2012).

In addition to micrographs, macrographs representing sample cross sections were helpful for clarifying the results. Fig. 8 compares cross sections of EPI and PRF-made LVL after exposure to 24 VPSD cycles where we observed cracks across this thickness direction of the veneers. These swelling cracks are likely caused by drying cycles, promoted by greater swelling in the tangential direction, and form along weak ray cells with crack normal in the tangential direction (Vasic and Stanzl-Tschegg 2007). They are

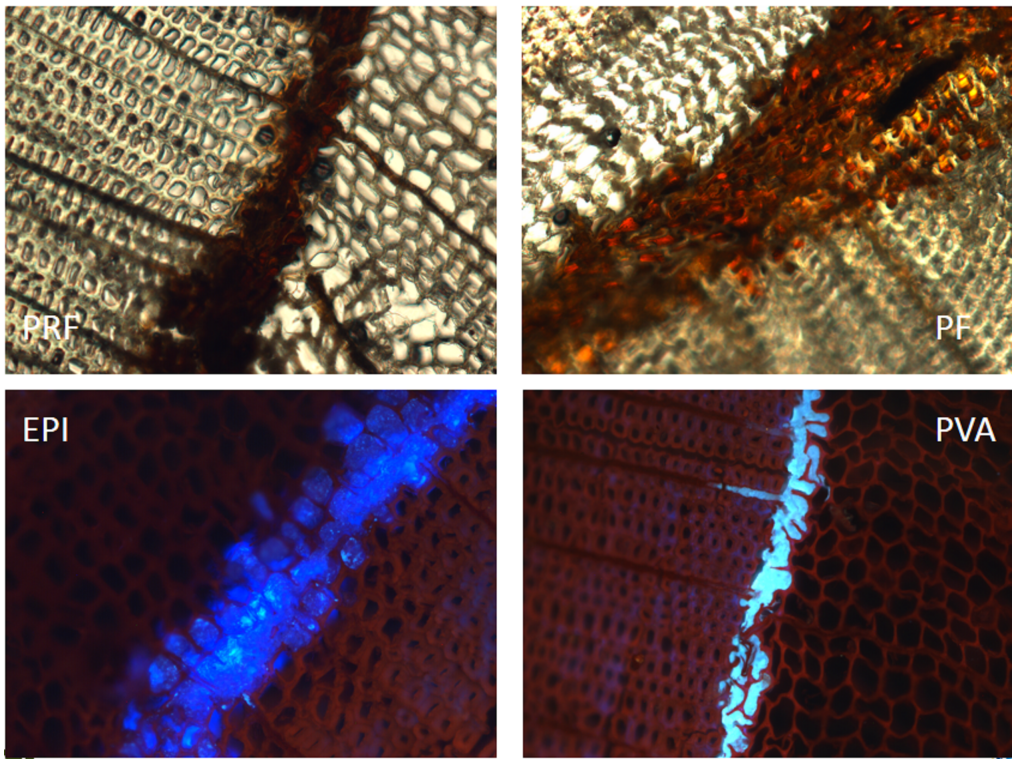

Figure 7: Micrographs of bond lines of various adhesives and Douglas fir substrate obtained with bright filed microscopy for PRF and PF (top) and UV microscopy after Safranin staining for EPI and PVA (bottom). 10X magnification.

across the thickness of the veneers because in rotary peeled veneers, the tangential direction of the wood is in the plane of the veneer. Because the crack normal of the drying cracks is the same as the crack normal in TL fracture tests, it is expected that formation of drying cracks will show up as degradation in TL fracture toughness. As a consequence, an adhesive's ability to distribute shrinkage and swelling stresses during aging could considerably affect swelling crack formation and that effect would be reflected in TL toughness.

Because these experiment were intended to characterize overall durability, rather than focus on bond lines alone, our fracture tests were mostly in the TL direction Experimental results show that TL fracture was affected more by the adhesive then RL fracture and therefore is the preferred mode for characterizing the role of the adhesive (Mirzaei *et al*, 2015). Possible interactions between TL and swelling-induced cracks with normal in the tangential direction provide additional support for using TL fracture. In contrast, RL crack growth (when used) often deviates into wood and would interact less with tangential swelling cracks. RL fracture would interact with swelling cracks with their normal in the radial direction, but our microscopy indicates that such swelling cracks are absent or at least much less common than tangential swelling cracks. In other words, RL fracture tests, like shear strength tests, are not expected to be informative about adhesive quality.

Conclusions

R curves of LVL samples made out of Douglas-fir and various wood adhesives were constructed with data from DCB fracture tests before and after exposure to cyclic accelerated aging, and the contribution of adhesives to the

material durability was investigated. Comparing average G_{ss} of LVL samples reflects the capability of crack propagation fracture toughness to distinguish different adhesive systems in terms of their durability, while the results of conventional test methods do not reveal such capability. Kinetics analysis of R curves was carried out to further investigate the correlation of durability and adhesives. The results demonstrate quantitative comparison of degradation rates of different adhesives after some crack propagation. Contrary to test methods that do not consider post-peak load regimes, crack propagation fracture toughness seems to be a promising tool for ranking and differentiating wood adhesives for their ability to make durable wood composites.

Acknowledgements: Financial support was provided by the National Science Foundation Industry/University Cooperative Research Center for Wood-Based Composites, Award No. IIP-1034975. We thank Momentive® Specialty Chemicals and Georgia Pacific Chemicals® for supplying all adhesives and veneer materials.

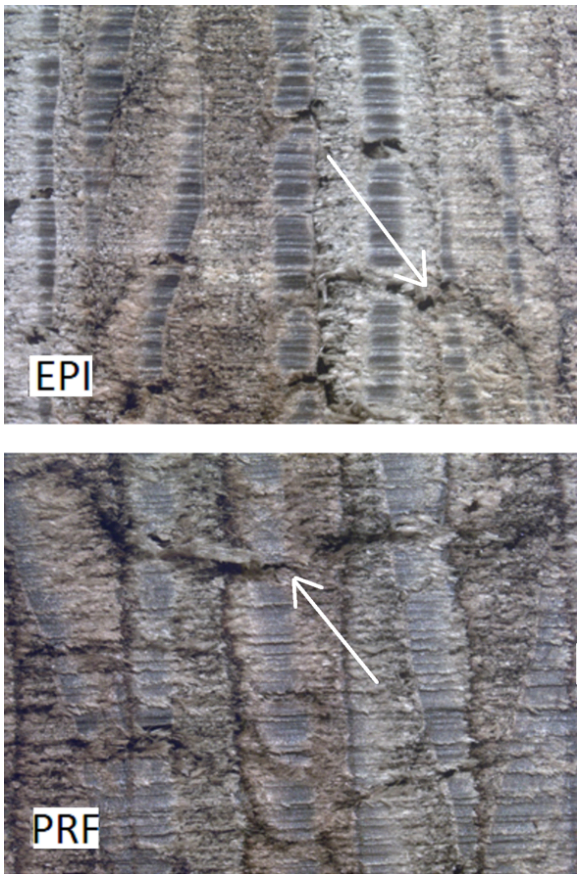

Figure 8: Crack formation in TR direction of EPI (top) and PRF (bottom) LVL due to aging.

References

Adamopoulos, S., Bastani, A., Gascon-Garrido, P., Militz, H., Mai, C. (2012) Adhesive bonding of beech wood modified with a phenol formaldehyde compound. *Eur. J. Wood Prod.* 70 (6): 897-901.

ASTM Standard (2012) D2559. Standard Specification for Adhesives for Bonded Structural Wood Products for Use Under Exterior Exposure Conditions.

ASTM Standard (2012) D1037. Standard Test Methods for Evaluating Properties of Wood-Base Fiber and Particle Panel Materials.

Follrich, J., Stockel, F., Konnerth, J. (2010) Macro- and micromechanical characterization of wood adhesive bonds exposed to alternating climate conditions. *Holzforschung* 64: 705–711,

Gallops, S. (2011) Development and Validation of a Fatigue Reliability Method for Bridging Materials (PhD thesis). *PhD thesis*, Oregon State University, Corvallis: Oregon State University.

Han, M. H., Nairn, J. A. (2003) Hygrothermal Aging of Polyimide Matrix Composite. *Composites Part A* 34: 979-986.

Hashemi, S., Kinloch, A. J. Williams, J. G. (1990) The Analysis of Interlaminar Fracture in Uniaxial Fibre-Polymer Composites. *Proc. R. Soc. Lond. A* 427: 173-199.

Irwin, G. R., Kies, J. A., & Smith, H. L. (1958). Fracture strengths relative to onset and arrest of crack propagation. *Proc. ASTM* 58: 640-657.

Kamke, F. A., Nairn, J. A., Muszynski, L., Paris, J. L., Schwarzkopf, M., Xiao, X. (2014) Methodology for micromechanical analysis of wood adhesive bonds using X-ray computed tomography and numerical modeling. *Wood and Fiber Science* 46 (1): 15-28.

Kim, H. W., Grayson, M. A., Nairn, J. A. (1995) The effect of hygrothermal aging on the microcracking properties of some carbon fiber/polyimide laminates. *Advanced Composites Letters* 4: 185-188.

Kojima, Y., Shigehiko, S. (2011) Evaluation of wood-based panel durability using bending properties after accelerated aging treatments. *J Wood Sci* 126–133.

Liswell, B. (2004) Exploration of Wood DCB Specimens Using Southern Yellow Pine for Monotonic and Cyclic Loading. *Masters thesis,* Blacksburg: Virginia Polytechnic Institute and State University.

MacLean, J. D. (1953) Effect of steaming on the strength of wood. *American Wood-Preservers' Association.*

Matsumoto, N., Nairn, J.A. (2012) Fracture Toughness of Wood and Wood Composites During Crack Propagation. *Wood and Fiber Science* 44: 121-133.

Mirzaei, B., Sinha, A., Nairn, J. A. (2015) Using Crack Propagation Fracture Toughness to Characterize the Durability of Wood and Wood Composites. *Materials and Design* 87: 586-592.

Nairn, J. A. (2009) Analytical and Numerical Modeling of R Curves for Cracks with Bridging Zones. *International Journal of Fracture* 167-181.

NIST Standard (2010). Voluntary Product Standard PS1 Structural Plywood.

Pizzi, A., Mittal, K. A. *Handbook of Adhesive Technology.* Marcel Dekker, Inc. New York, 2003.

Sinha, A., Nairn, J. A., Gupta, R. (2012) The effect of elevated temperature exposure on the fracture toughness of solid wood and structural wood composites. *Wood Sci Technol* 46: 1127–1149.

Sinha, A., Gupta, R., Nairn, J. A. (2011) Thermal degradation of bending properties of structural wood and wood-based composites. *Holzforschung* 65 (2): 221-229.

Smith, I., Landis, E., Gong, M., *Fracture and Fatigue in Wood.* Wiley. Chichester, 2003.

Stoeckel, F., Konnerth, J., Gindl-Altmutter, W. (2013) Mechanical properties of adhesives for bonding wood—A review. *International Journal of Adhesion & Adhesives* 45: 32–41.

Suzuki, M., Schniewind, A. P. (1987) Relationship between fracture toughness and acoustic emission during cleavage failure in adhesive joints. *Wood Science and Technology* 21 (2): 121-130 .

US Forest Products Laboratory. *Wood handbook: wood as an engineering.* United States Government Printing. Madison, 2010.

Vasic, S., Stanzl-Tschegg, S. (2007) Experimental and numerical investigation of wood fracture mechanisms at different humidity levels. *Holzforschung* 61 (4): 367–374.

Wang, B. J., Dai, C. (2005). Hot-pressing stress graded aspen veneer for laminated veneer lumber (LVL). *Holzforschung*, 59(1), 10-17.